doi: 10.56761/EFRE2022.S1-O-051301

# Irradiation effect of intense pulsed ion beam on (TiZrNbTaCr)C

*S.J. Zhang[1,2,3], L. Chen[4], A.V. Stepanov[3], O.P. Lapteva[3], G.E. Kholodnaya[3], X. Yu[1,2], M.F. Xu[1,2], Y.J. Wang[4], G.E. Remnev[3], X.Y. Le[1,2,*]*

[1]*Beihang University, Beijing, China*
[2]*Ministry of Industry and Information Technology, Beijing, China*
[3]*National Research Tomsk Polytechnic University, Tomsk, Russia*
[4]*Harbin Institute of Technology, Harbin, China*
[*]*xyle@buaa.edu.cn*

**Abstract.** Intense pulsed ion beam (IPIB), featured with pulsed high-power density, has been widely used in the modification of materials. The influence of IPIB irradiation on surface microstructure and phase structure of (TiZrNbTaCr)C ceramics was investigated in this work. Experiments were carried out using TEMP-4M accelerator with peak accelerating voltage, current density, and pulse duration (FWHM) of 220 kV, 150 A/cm$^2$, and 80 ns respectively. Atomic force microscope (AFM), scanning electron microscope and Energy-dispersive X-ray spectroscopy (SEM-EDS), as well as X-ray diffraction (XRD) were used to analyze the surface microstructure and phase structure of (TiZrNbTaCr)C ceramics under IPIB irradiation. The AFM and SEM images showed that the grain size of (TiZrNbTaCr)C increased, and the size and quantity of holes decreased after IPIB irradiation which might improve the erosion resistance of material. After IPIB irradiation, the segregation of Cr and Ta elements were observed by EDS measurement. The phase structure stability of samples under IPIB irradiation was confirmed by XRD and the lattice parameters and crystal spacing was discussed as well.
**Keywords:** high entropy ceramics, intense pulse ion beam, irradiation effect, microstructure.

## 1. Introduction

Intense pulsed ion beam (IPIB), invented as ignition technique for inertial confinement fusion (ICF) [1], has been intensively researched for various applications such as nanopowder synthesis [2, 3], film deposition [4, 5], surface modification [6, 7] and simulation of high thermal load for nuclear fusion [8]. When IPIB with high-power density bombard on material, a fast temperature rise and decline are induced in the near-surface region of material, giving rise to melting, evaporation, and re-solidification. Consequently, the microstructure and properties of material in near-surface region can be changed. Meanwhile, the thermal stress and shock wave generated by IPIB may influence the mechanical properties in deeper region [9, 10].

The high entropy materials have attracted great attention due to its remarkable properties including high mechanical strength, high-temperature strength and good corrosion and oxidation resistance [11]. In recent years, high entropy carbides (HECs) have drawn considerable research interest due to their promising properties and potential application in extreme environments [12–14].

In this work, the surface morphology, elemental distribution and phase structure of (TiZrNbTaCr)C ceramic under pulsed intense thermal effect were investigated by IPIB irradiation. The experimental results provide useful information to the future studies on the application of HECs in extreme conditions and the practical utilization of IPIB in material modification.

## 2. Experimental

The IPIB irradiation experiments were carried out using the TEMP-4M accelerator at Tomsk Polytechnic University. The main ion species of IPIB produced by TEMP-4M are around 85% of carbon ions and 15% of hydrogen ions [15]. The accelerating voltage and current density were measured by voltage divider and Faraday cup. In this experiment, the working accelerating voltage and current density of IPIB are around 220 kV and 150 A/cm$^2$, as shown in Fig.1. The pulse duration FWHM (full width at half-maximum) of IPIB is about 80 ns.

The high entropy (TiZrNbTaCr)C ceramic was used as sample in this work. The design and preparation of (TiZrNbTaCr)C ceramic was completed by School of Materials Science and

Engineering, Harbin Institute of Technology. The ceramic was polished before being irradiated by IPIB and its dimension was 19×19×1 $mm^3$. The sample was placed vertically in the beam path for IPIB irradiation. The sample was divided into three areas by a copper plate and the two of these three areas were irradiated by IPIB with 5 and 45 pulses respectively. The time interval between pulses was around 10 s.

The phase structure of sample before and after IPIB irradiation was detected by X-ray diffraction (XRD, XRD-7000S) with Cu Kα radiation source operated at 40 kV and 30 mA. The surface morphologies of sample were observed by atomic force microscopy (AFM, NtMdt Integra Prima) and scanning electron microscopy (SEM, JSM-7500FA). The elemental compositions of sample before and after IPIB irradiation were detected by energy dispersive X-ray spectroscopy (EDS).

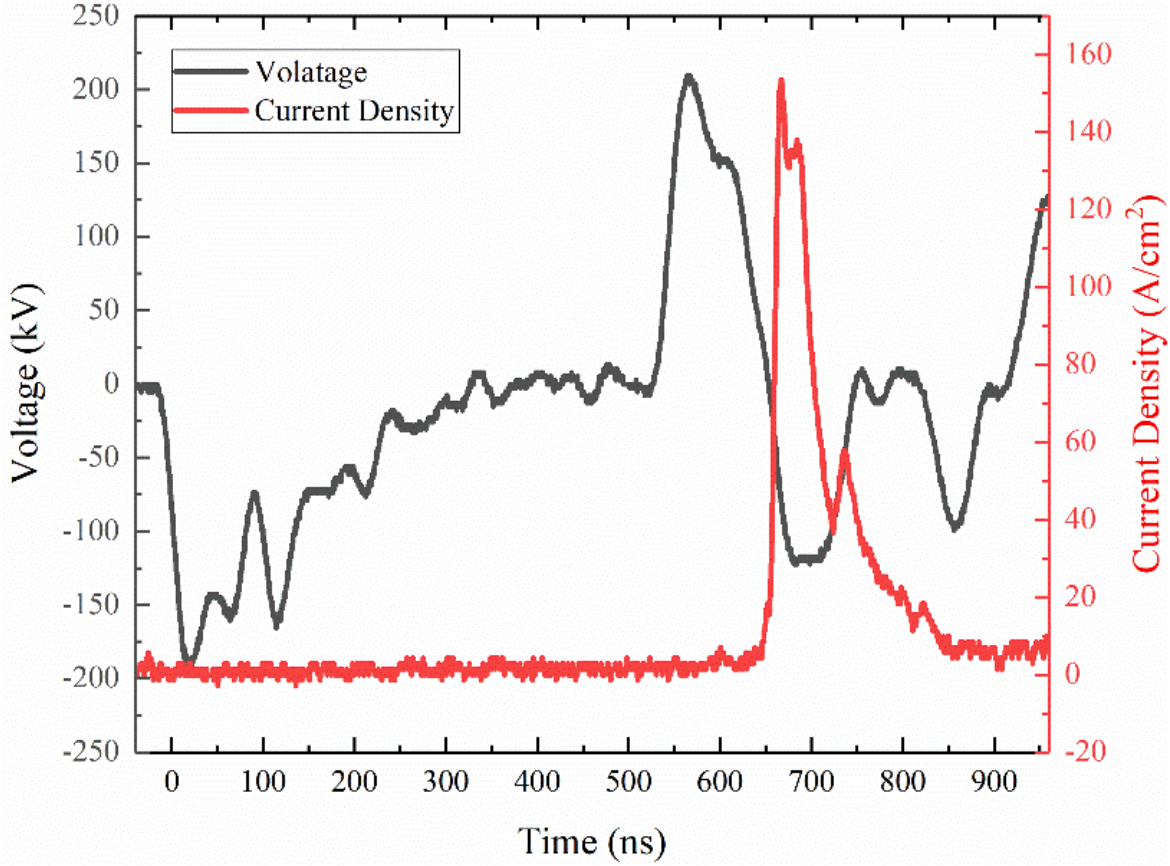


Fig.1. Accelerating voltage and current density of TEMP-4M accelerator.

## 3. Experimental results

*3.1. Surface morphology and elemental distribution*

The optical image of sample after IPIB irradiation with different pulses is shown in Fig.2. It is obvious that the color of surface of (TiZrNbTaCr)C ceramic turns out to be much brighter after IPIB irradiation.

The 3D and corresponding 2D AFM images of (TiZrNbTaCr)C ceramic treated by different pulses of IPIB are shown in Fig.3. Small grains and some holes can be observed on the surface of original sample (Fig.3a). Two main changes occurred after IPIB irradiation, i.e. the grain size increased obviously and the surface became much denser with the disappearing of holes, as shown in Fig.3b and 3c. The dense surface might benefit to enhance material properties, such as corrosion resistance, due to the less corrosion route into the bulk of material. The surface topography and roughness increased due to the bigger grain size.

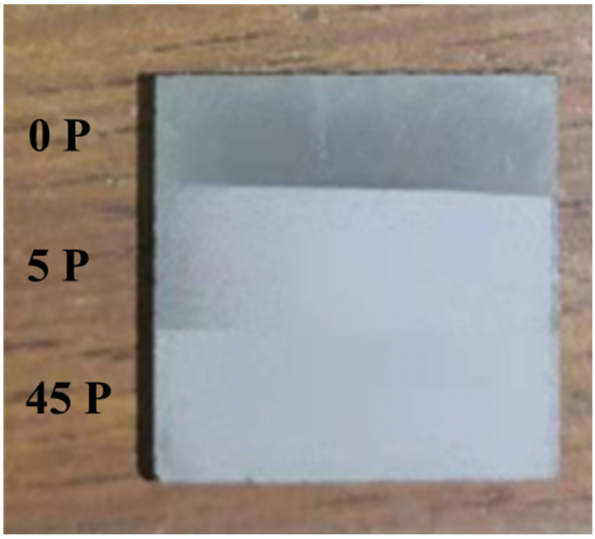


Fig.2. Optical image of sample after IPIB irradiation with different pulses.

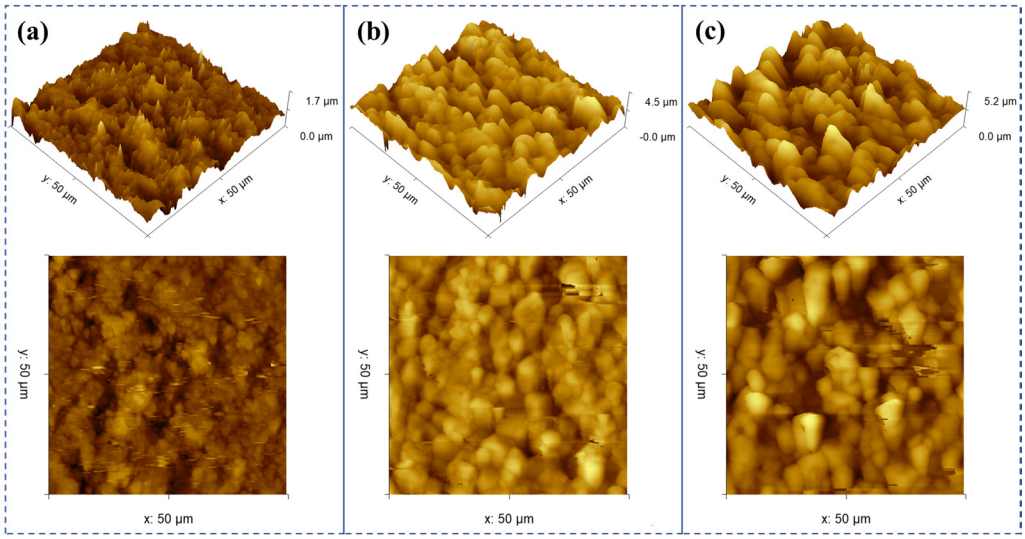


Fig.3. AFM images for samples with different pulses IPIB irradiation: (a) – original, (b) – 5 pulses, (c) – 45 pulses. The upper is 3D profile and lower is corresponding 2D profile.

The SEM morphology and corresponding EDS elemental mapping of (TiZrNbTaCr)C ceramic with different IPIB irradiation are shown in Fig.4. Some cracks and holes appeared on the surface of original sample which might be caused due to the incomplete densification [16], as shown in Fig.4a. The grain of original sample is irregular and small. After IPIB irradiation, the grain size increased which is consistent with AFM observation and cracks disappeared. Subsequently, the size and number of holes decreased as shown in Fig.4b and 4c. The mass transport and convection would occur in the liquid state of near-surface region of sample caused by IPIB [17], which might be the reason for the grain increment and defects decrement. The grain shape of sample with 45 pulses is flatter than that of sample with 5 pulses IPIB irradiation. The repeat surface tension might be attribute to the flatter shape of grain in case of 45 pulses IPIB irradiation [18].

The elemental distribution changed after IPIB irradiation, as shown in Fig.4. The segregation of Cr element is obvious and Ta element also has slight segregation as shown in Fig.4b and 4c. The elemental component of sample after different pulses IPIB irradiation is summarized in Fig.5. The other elements decrease to the half after 5 pulses and keep decreasing to trace after 45 pulses of IPIB irradiation. The intense thermal effect might cause the evaporation or ablation of the contaminants,

which leads to the decrease of other elements. After IPIB irradiation, the amount of main metal elements increases and changes little with more pulses. However, the ratio of five main metal elements (Ti, Zr, Nb, Ta, Cr) keeps similar before and after IPIB irradiation.

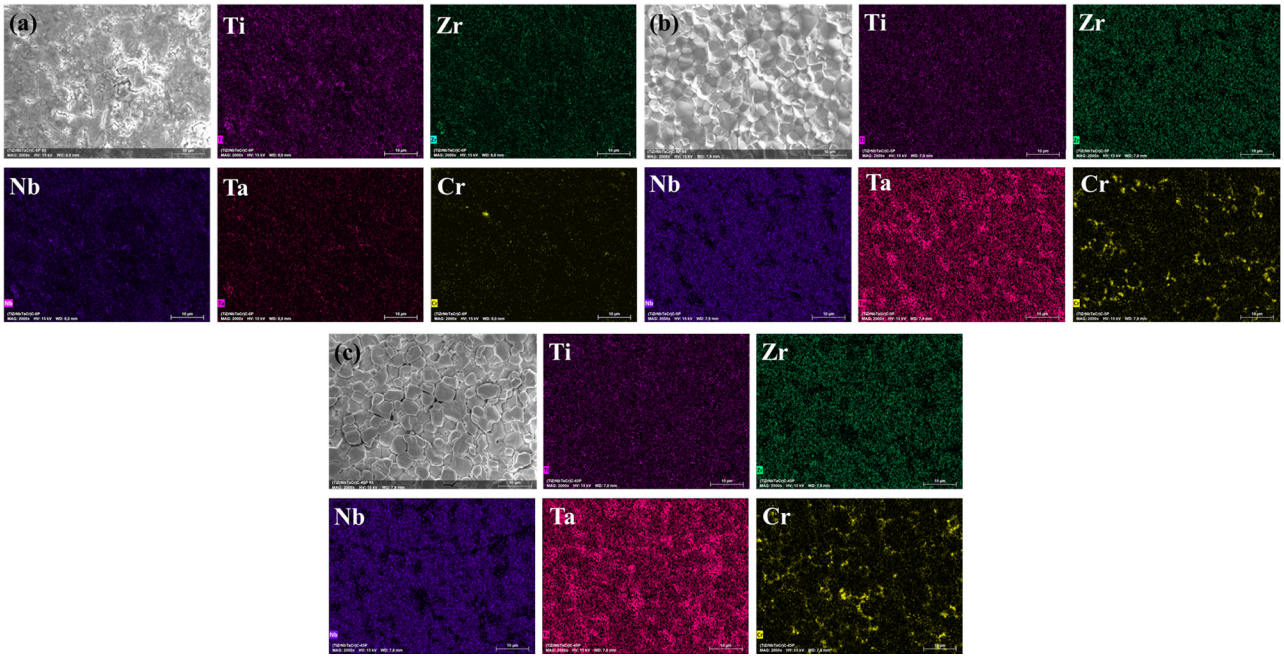


Fig.4. SEM images with corresponding elements mapping of Ti, Zr, Nb, Ta and Cr element of sample with different pulses of IPIB irradiation: (a) – original, (b) – 5 pulses, (c) – 45 pulses.

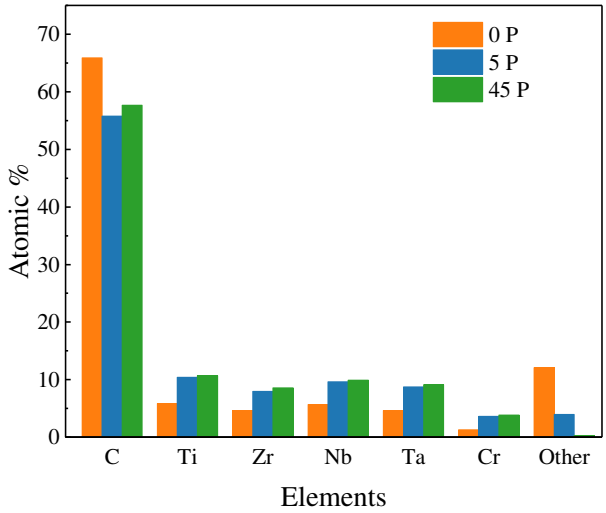


Fig. 5. Elemental component of each mapping in Fig 4.

*3.2. Phase structure*

The XRD measurements were made to detect the phase structure of (TiZrNbTaCr)C ceramic with different IPIB irradiation treatments, as shown in Fig.6. The XRD patterns indicate that the (TiZrNbTaCr)C ceramic has a face-centered cubic (FCC) structure and there is no phase change after IPIB irradiation, as shown in Fig.6a. The peak position of XRD patterns shifts to left slightly after IPIB irradiation, which means that the crystalline spacing increases a little according to Bragg law. The lattice constant was calculated by Jade 6.5 software which are 4.47267 Å, 4.47518 Å and 4.47428 Å for original, 5 pulses and 45 pulses IPIB treatments samples respectively.

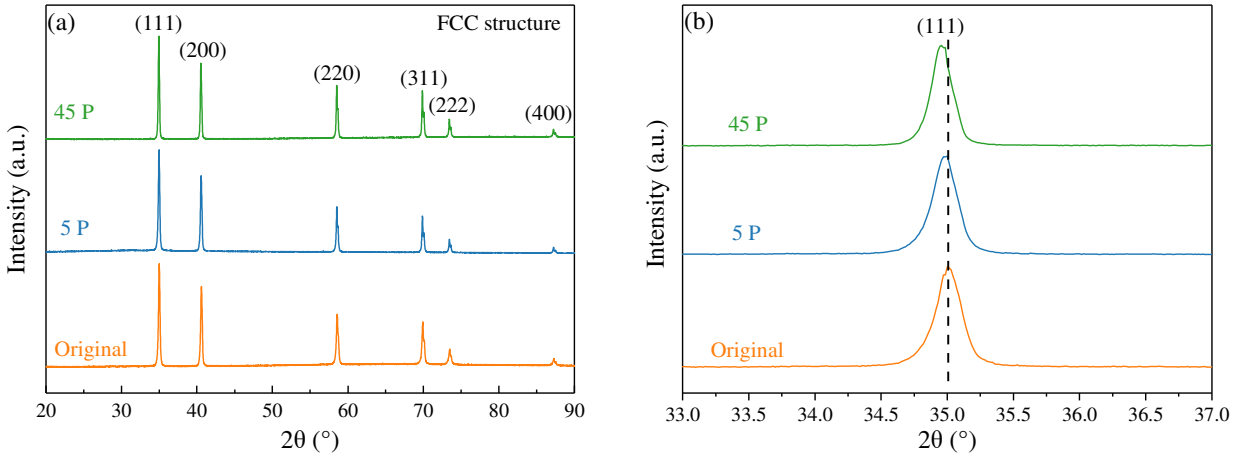


Fig.6. (a) – XRD patterns of (TiZrNbTaCr)C ceramic with different IPIB irradiation treatments, (b) – enlarged XRD pattern of (111).

## 4. Conclusion

The surface morphology and phase structure of high entropy ceramic (TiZrNbTaCr)C before and after IPIB irradiation were experimental analyzed. After IPIB irradiation, the grain size of (TiZrNbTaCr)C ceramic increased, and the shape of grain became flatter with more pulses of treatment. The surface defects, like cracks and holes, mostly disappeared after IPIB irradiation. The oxygen and other elements on the surface of (TiZrNbTaCr)C ceramic were mostly removed by IPIB irradiation. The segregation of Cr and Ta elements was formed under IPIB irradiation. The crystal spacing of (TiZrNbTaCr)C ceramic increased slightly but its FCC structure kept stable under IPIB irradiation.

## Acknowledgments

The reported research was funded by NSFC, Contract No. 11875084 and 12075024, and joint project of RFBR and NSFC, Contract No. 21-53-53013.

The SEM measurement in this research was carried out using the equipment of the Center for Sharing Use «Nanomaterials and Nanotechnologies» of Tomsk Polytechnic University supported by the RF Ministry of Education and Science project #075-15-2021-710. The authors are grateful to Mr. S. Pavlov from Tomsk Polytechnic University for his help in AFM measurement.

## 5. References

[1] Humphries S., *Nucl. Fusion.*, **20**, 1549, 1980; doi: 10.1088/0029-5515/20/12/006

[2] Yatsui K., Grigoriu C., Kubo H., Masugata K., Shimotori Y., *Appl. Phys. Lett.*, **67**, 1214, 1995; doi: 10.1063/1.115011

[3] Remnev G.E., Uglov V.V., Shymanski V.I., Konarski P., Samtsov M.P., Pavlov S.K., Lapchuk N.M., *Vacuum*, **89**, 118, 2013; doi: 10.1016/j.vacuum.2012.02.037

[4] Mei X.X., Xu J., Ma T.C., *Wuli Xuebao/Acta Phys. Sin.*, **51**, 1880, 2002;

[5] Sonegawa T., Grigoriu C., Masugata K., Yatsui K., Shimotori Y., Furuuchi S., Yamamoto H., *Appl. Phys. Lett.*, **69**, 2193, 1996; doi: 10.1063/1.117162

[6] Zhang Q., Mei X., Guan T., Zhang X., Remnev G.E., Pavlov S.K., Wang Y., *Fusion Eng. Des.*, **138**, 16, 2019; doi: 10.1016/j.fusengdes.2018.10.012

[7] Romanov I.G., Tsareva I.N., *Tech. Phys. Lett.*, **27**, 695, 2001; doi: 10.1134/1.1398972

[8] Zou H., Zhang L., Guan T., Zhang X., Remnev G.E., Pavlov S.K., Wang Y., Mei X., *Surf. Coatings Technol.*, **384**, 125333, 2020; doi: 10.1016/j.surfcoat.2020.125333

[9] Yan S., Le X.Y., Zhao W.J., Han B.X., Xiang W., Wang Y.G., Xue J.M., *Nucl. Tech.*, **26**, 217, 2003.
[10] Shulov V.A., Nochovnaya N.A., Remnev G.E., *Mater. Sci. Eng. A*., **243**, 290, 1998; doi: 10.1016/s0921-5093(97)00816-2
[11] Tsai M.H., Yeh J.W., *Mater. Res. Lett.*, **2**, 107, 2014; doi: 10.1080/21663831.2014.912690
[12] Zhang W., Chen L., Xu C., Lu W., Wang Y., Ouyang J., Zhou Y., *J. Mater. Sci. Technol.*, **72**, 23, 2021; doi.org/10.1016/j.jmst.2020.07.019
[13] Wang Y., Zhang B., Zhang C., Yin J., Reece M.J., *J. Mater. Sci. Technol.*, **113**, 40, 2022; doi: 10.1016/j.jmst.2021.09.064
[14] Chen L., Wang K., Su W., Zhang W., Xu C., Wang Y., Zhou Y., *Wuji Cailiao Xuebao/Journal Inorg. Mater.*, **35**, 748, 2020; doi: 10.15541/jim20190408
[15] Zhang J., Zhong H., Shen J., Yu X., Yan S., Le X., *Surf. Coatings Technol.*, **388**, 125599, 2020; doi: 10.1016/j.surfcoat.2020.125599
[16] Wang K., Chen L., Xu C., Zhang W., Liu Z., Wang Y., Ouyang J., Zhang X., Fu Y., Zhou Y., *J. Mater. Sci. Technol.*, **39**, 99, 2020; doi: 10.1016/j.jmst.2019.07.056
[17] Yan S., Le X.Y., Zhao W.J., Shang Y.J., Wang Y., Xue J., *Surf. Coatings Technol.*, **201**, 4817, 2007; doi: 10.1016/j.surfcoat.2006.07.028
[18] Yu X., Shen J., Zhong H., Zhang J., Yan S., Zhang G., Zhang X., Le X., *Vacuum*, **120**, 116, 2015; doi: 10.1016/j.vacuum.2015.06.028